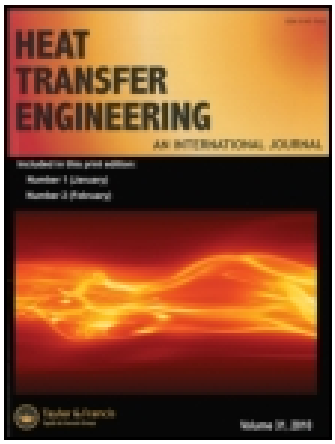

Heat Transfer Engineering
Publication details, including instructions for authors and subscription information:
http://www.tandfonline.com/loi/uhte20

A Honeycomb Microchannel Cooling System for Microelectronics Cooling

Xiaobing Luo [a] , Yonglu Liu [a b] & Wei Liu [a]
[a] School of Energy and Power Engineering , Huazhong University of Science and Technology , Wuhan, China
[b] Department of Mechanical and Power Engineering , Nanchang Institute of Technology , Nanchang, China
Published online: 16 Nov 2011.

To cite this article: Xiaobing Luo , Yonglu Liu & Wei Liu (2011) A Honeycomb Microchannel Cooling System for Microelectronics Cooling, Heat Transfer Engineering, 32:7-8, 616-623, DOI: 10.1080/01457632.2010.509755

To link to this article: http://dx.doi.org/10.1080/01457632.2010.509755

Heat Transfer Engineering, 32(7–8):616–623, 2011

ISSN: 0145-7632 print / 1521-0537 online
DOI: 10.1080/01457632.2010.509755

Taylor & Francis
Taylor & Francis Group

A Honeycomb Microchannel Cooling System for Microelectronics Cooling

XIAOBING LUO,[1] YONGLU LIU,[1,2] and WEI LIU[1]

[1]School of Energy and Power Engineering, Huazhong University of Science and Technology, Wuhan, China
[2]Department of Mechanical and Power Engineering, Nanchang Institute of Technology, Nanchang, China

A honeycomb porous microchannel cooling system for electronics cooling was proposed in this article. The design, fabrication, and test system configuration of the microchannel heat sink were summarized. Preliminary experimental investigation was conducted to understand the characteristics of heat transfer and cooling performance under steady single-phase flow. In the experiments, a brass microchannel heat sink was attached to a test heater with 8 cm^2 area. The experimental results show that the cooling system is able to remove 18.2 W/cm^2 of heat flux under 2.4 W pumping power, while the junction wall temperature is 48.3°C at the room temperature of 26°C. Extensive experiments in various operation conditions and parameters for the present cooling system were also conducted. The experimental results show that the present cooling system is able to perform heat dissipation well.

INTRODUCTION

Recent advances in micro electromechanical devices (MEMS), very large-scale integration (VLSI) technologies, and the associated micro miniaturizations have led to significant increases in the packaging densities and heat fluxes generated within these devices. To operate electronic devices at a suitable temperature, it is necessary to develop efficient heat removal methods. One possible solution is to utilize microchannel heat sinks, structures with which many microscale channels of large-aspect ratios are built onto the back of the microchips. Working liquid is forced through these microchannels to carry away the heat. This approach was first introduced by Tuckerman and Pease 28 years ago [1]. Since the original study, numerous investigations have been conducted using a variety of techniques, as reviewed by Phillips [2].

According to Newton's law of cooling, two conventional strategies can be employed to improve the forced conventional heat transfer rate under specified temperature differences. One strategy involves extending the surface area of a heat sink. Due to their compactness and high surface-to-volume ratio, the use of microchannels seems an attractive method. However, the high packaging density in advanced electronic chips limits the infinite extension of the surface area of the heat sink. The other strategy is the enhancement of the heat transfer coefficient. Traditionally, flow disturbance technologies using roughness elements, vortex, etc., may help to increase the heat transfer coefficient in single-phase laminar flow.

While microchannel heat exchangers generally have excellent thermal performance, there is still considerable emphasis on increasing heat transfer coefficients. The use of enhanced microchannels was proposed by Kishimoto and Sasaki [3]. They proposed a diamond-shaped interrupted microgrooved cooling fin to decrease junction temperature variations across the chip. It was found that the high heat transfer coefficient could be obtained by interrupting the thermal boundary layer with cooling fins in a staggered arrangement.

Steinke and Kandlikar [4] have carried out an extensive review of conventional single-phase heat transfer enhancement techniques. Several passive and active enhancement techniques for minichannels and microchannels were discussed. Some of their proposed enhancement techniques included fluid additives, secondary flows, vibrations, and flow pulsations. Kandlikar and Upadhye [5] analyzed the enhanced offset strip-fin geometry, with the results showing that by using water as the coolant in a split-flow arrangement with a core pressure drop of around 35 kPa, the enhanced structures were capable of dissipating heat fluxes extending beyond 3 MW/m^2.

The authors give thanks for the financial support from 973 Project of the National Science and Technology Ministry of China (2009CB320203).

Address correspondence to Dr. Xiaobing Luo, State Key Laboratory of Coal Combustion, School of Energy and Power Engineering, Huazhong University of Science and Technology, Wuhan, China 430074. E-mail: Luoxb@mail.hust.edu.cn

Some researchers have focused on honeycomb structures for augmenting heat transfer in compact heat exchangers. According to the report of Lu [6], the surface area to volume ratio of the typical micro-cell at the size of 1-mm aluminum honeycombs was about 3000 m^2/m^3, making them ideal candidates for compact heat exchanger applications where high surface area density is required.

Honeycomb structures metals are low-density materials that combine a certain stiffness, strength, crushing energy absorption, and thermal characteristics. With a single "easy flow" direction to allow internal fluid transportation, the continuous channels of these open core structures make them particularly interesting for use in heat sink applications. For these reasons, all-metallic sandwich structures with honeycomb cores have been suggested for simultaneous load bearing and active cooling [7]. Several mechanisms contributing to heat transfer have been identified, including a high surface contact area between the core and the coolant, and high heat transfer between the metal surface and the fluid coolant [8–10]. Experimental studies of convective heat transfer in extruded metallic honeycomb structures have been performed by Hayes et al. [11] and Dempsey et al. [12]. The test heat sinks were fabricated as sandwich panels with honeycomb cores bonded to two solid face-sheets by welding, three sides insulated, and the top or bottom surface subjected to prescribed temperatures or heat flux, using forced air as the coolant for the cross-flow heat exchange experiments. Exel and Schulz-Harder [13] provided a honeycomb microchannel design based on the diffusion bonding process; the system has good cooling performance, but it is expensive because of such a fabrication process.

Based on previous studies, an improved design for periodic staggered honeycomb structure microchannel heat sinks and a cooling system for them are presented in this article. The design, fabrication, and test system configuration of the microchannel heat sink are summarized. A parametric experimental study on the cooling systems was conducted. The experimental results show that the present cooling system is able to perform well.

HEAT SINK DESIGN

The prototypical structure of the multilayer honeycomb heat sink is built by stacking together several flat thin rectangle metal plates with etched honeycomb holes inside to form the staggered fluid flow passage channels. As shown in Figure 1a and b, each of the metal plates has the same size of $L \times W \times H$, which is etched so that it has a number of small regular hexagonal honeycomb cells with ex-circle diameter d and fin thickness t. In order to keep the two layers tightly connected, a wide seal region a with no honeycomb cells is left around the perimeter of the metal plate. By rotating one plate at a 180° angle going clockwise and then bonding with the other plate, the honeycomb holes are divided by cell fins to form the serpentine fluid

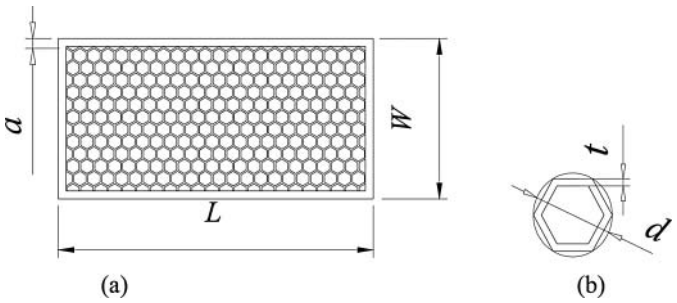

Figure 1 The prototype of a single layer honeycomb plate.

flow channels in the direction of a normal layer plane, as shown in Figure 2. The heat sink inner structure is simply created by stacking multilayered honeycomb microchannel plates together. For applications of indirect liquid cooling of electronic systems, the working liquid is forced to flow through well-designed channels embedded in the cellular metal core in order to realize heat dissipation.

The dimensions of the hexagonal honeycomb cells are controlled primarily by metal etching methods, with chemical etching on the unprotected metal material. In contrast to the traditional machination process, the etching method has a short production cycle of about several days. Chemical etching is extremely flexible, and for any applications needed, any pattern can be copied onto the metal. This method also works well for changing dimensions; chemical etching is able to do this more quickly and easily than other methods. Finally, and perhaps most importantly, the development cost is low. A sample of a fabricated honeycomb microchannel plate is shown in Figure 3 and the multilayered sample is shown in Figure 4.

The configuration of the staggered honeycomb microchannel heat sink is illustrated in Figure 5. The heat sink and the channels are made of brass (H62). Each heat sink is composed of 15 honeycomb layers, where each individual layer has dimensions of $40 \times 20 \times 0.16$ mm. Rows of regular hexagonal honeycomb cells in the flat thin brass plate also have the same dimensions of cell, ex-circle diameter of 2.49 mm and fin width of 0.2 mm. As seen from Figure 2, when stacking multilayered honeycomb microchannel plates together, each honeycomb cell is divided into three smaller parts by the cell fins in the neighbor layering, forming serpentine microchannels. To reduce contact

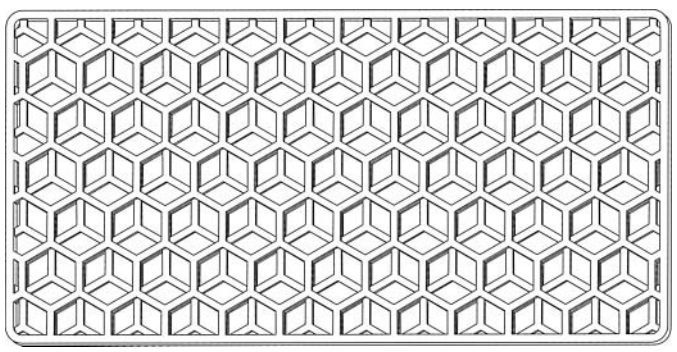

Figure 2 Two honeycomb plates bonded together.

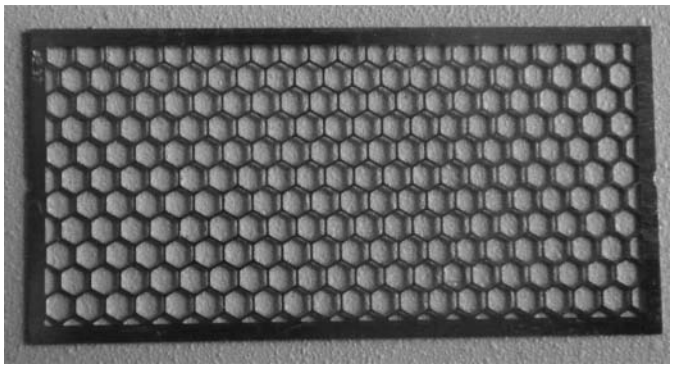

Figure 3 Fabricated sample of a single layer plate.

thermal resistance, multilayers of these honeycomb plates are bonded together through the 14 laser welding lines in the side region around the perimeter of the plates, as shown in Figure 4. The thermal resistance can thus be minimized by the many contact points between the metal layers. The chamber containing the honeycomb microchannel structure is bonded with a cover board with inlet/outlet pipes at the top of the channels using miniature "O-rings" for fluidic sealing.

In this honeycomb microchannel heat sink design, not only is the surface area expected to expand, but the flows are also modified to enhance heat transfer in a cost-effective way.

SYSTEM AND EXPERIMENTAL DESCRIPTION

Figure 6 demonstrates the closed-loop honeycomb porous microchannel cooling system for electronics cooling. It is composed of four parts: a microchannel heat sink, a micropump, a reservoir, and a small heat exchanger with a fan. When the electronic chips need to be cooled, the system starts to work. Water, or any other fluid in the closed system, is driven into the heat sink device through an inlet by a micropump. The inlet and outlet of the heat sink are located on the top of the heat transfer device, from which the fluid is directly pushed onto the bottom plate, which is attached to electronic chips. Since the honeycomb porous microchannel heat sink has a very large heat transfer coefficient, the heat created by electronic chips is easily

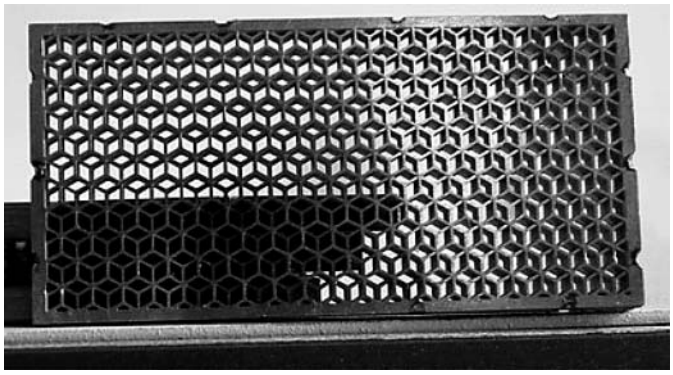

Figure 4 Multilayered plate bonded together.

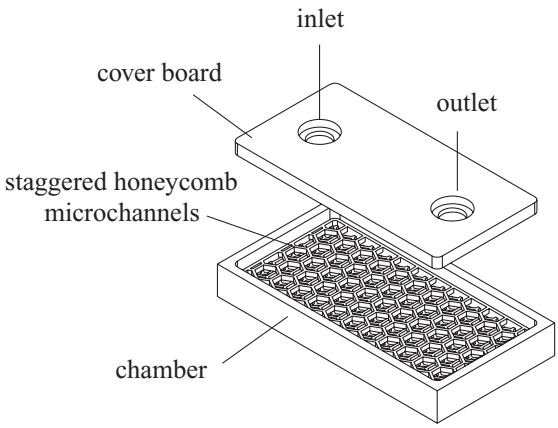

Figure 5 Schematics of a staggered honeycomb microchannel heat sink.

removed using the recycling fluid in the system. The fluid is then heated, with the temperature increasing after flowing out of the heat sink device. The heated fluid next enters the heat exchanger with the fins and fan. The heat exchanger will cool the fluid and the heat is dissipated into the external environment. The cooled fluid will be delivered into the reservoir to ensure that the fluid in the micropump is in liquid phase to keep the micropump working properly. From the low outlet of the reservoir, the cooled fluid is then pumped back into the heat sink, thus forming a closed-loop flow system. It should be noted here that the real size of the system can be designed as one small package, according to application requirements.

In the test system for this report, water was used as the working fluid. The heater, which was attached to the back of the device, was wired through electric pads to the power supply. In order to minimize heat loss, the external surface of the heating element and the heat sink were covered with a thermal insulation material with very low thermal conductivity (about 0.032 W/m-K).

In the experiment, temperature was the main parameter for system evaluation, and it was directly measured using T-type thermocouples (Cu–CuNi). Calibration of the thermocouples

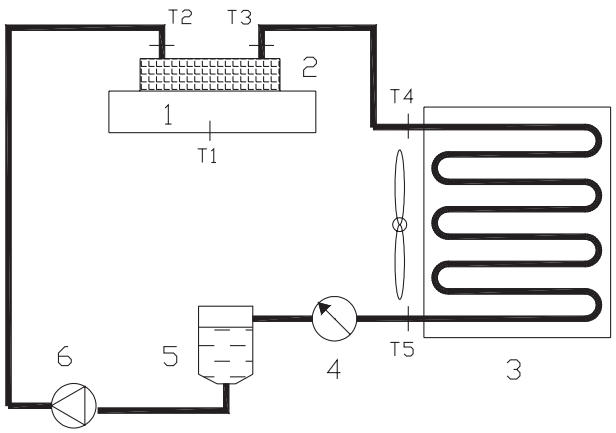

1. Heating system 2. Microchannel heat sink 3. Heat exchanger 4. Rotameter 5. Reservoir 6. Micropump T1-T5. T-type thermocouples

Figure 6 Schematic diagram of the experimental system.

was performed prior to the experiment by placing the device in an oven and establishing the resistance–temperature curve for each individual sensor. The uncertainty of the temperature measurement of the T-type thermocouples was ±0.2 K after calibration. The temperatures of the inlet and outlet fluids were measured by two thermocouples, one thermocouple T2 at the inlet and another T3 at the outlet of the test heat sink. The attached bottom wall surface temperature of the heat sink was measured using thermocouple T1, which was mounted on the back of the test sample. Thermocouples T4 and T5 were used to measure the temperatures of the in/out fluids of the heat exchanger. All these output signals of the thermocouple were recorded by a data acquisition system (Keithley 2700). The input heating power was controlled by the heating system, which was connected to a power supply with an adjustable AC voltage to provide power to the device. The uncertainty of the heating power measurement of the power meter was ±2W. The electrical voltage and current of the micropump were measured by the voltage meter with ±1 V uncertainty and the current meter with ±0.1 A uncertainty, respectively.

All measurements were performed under steady-state conditions and repeated until significant data repetition was ensured. The mass flow rate was controlled through adjusting the input voltage of the micropump. During the measurement, the pump and power source were set up to maintain a desired output. The pump was set up to produce a constant flow rate at a steady state.

During the experiments, the total volumetric flow rate $\dot{v}$ was also measured, with other parameters used to describe how the heat transfer and fluid flow characteristics of water were related to these measured parameters. The total heat steady-state transfer rate $\dot{Q}$ removed by water and the heat flux q at the bottom wall of the microchannel heat sink removed by water, respectively, are given by:

$$\dot{Q} = \dot{m} c_p \Delta T \tag{1}$$

$$q = \dot{Q} / A \tag{2}$$

where $\dot{m}$ is the total mass flow rate, c_p is the specific heat of the fluid, and ΔT is the temperature change. The mass flow rate is calculated by using the fluid density at the mean temperature and the measured volumetric flow rate. The temperature change is determined from the measured inlet and exit temperatures. A is the area of the bottom wall of the microchannel heat sink.

In order to evaluate the cooling system resistance, the power consumption of the micropump is also important for understanding the system. The electrical input power is determined by the following equation:

$$P = V I \tag{3}$$

where V is the input voltage and I is the input current.

Table 1 Dimensional details of the heat sinks

ID	L (mm)	W (mm)	H (mm)	a (mm)	t (mm)	d (mm)	D (mm)	n
I	40	20	0.2	3	0.2	2.27	2	8
II	40	20	0.16	1	0.2	2.49	4	15

RESULTS AND ANALYSIS

Performance Test

Tests were conducted at various input heating power levels. Figure 7 shows the variation of the measured heat sink temperature with time at different heat flux removed by the water at the same flow rate of micropump. Here, the flow rate of micropump was 463 mL/min. The electrical input voltage and current of the micropump were DC 12 V and 0.2 A, and thus the consuming power of the micropump was 2.4 W. The tests were initially started at a heating power of 80 W, and then stepped up to 90 W, 100 W, and 110 W. From Figure 7, it can be seen that when the input heating power was 80W, the inlet water fluid temperature T2 was 15.3°C, outlet temperature T3 was 17.8°C, and the bottom wall surface temperature of the heat sink T1 was 32.5°C, the total heat transfer rate $\dot{Q}$ removed by water was 75.2 W through the calculation of formula (1), and therefore, the heat flux q at the bottom wall of the microchannel heat sink removed by water was 9.4 W/cm^2 as shown in Figure 7a. When the input heating power increases to 150 W, as shown in the Figure 7b, the inlet water temperature T2 was 15.1°C, outlet temperature T3 was 20°C, and the bottom wall surface temperature of the heat sink T1 rose to 48.3°C, which is safe for normal electrical chips. In this case, the total heat transfer rate $\dot{Q}$ was 145.6W, and the heat flux q at the bottom wall of the microchannel heat sink removed by water was 18.2W/cm^2. From Figure 7b, it was also found that when the heating system stopped heating, temperature T1 of the bottom wall surface decreased rapidly.

Effect Investigations of Different Parameters on Cooling Performance

Extensive experiments under various operation conditions on the present cooling system were also conducted. Two test heat sinks were fabricated with different microchannel plate sizes and pipe diameters. The detailed dimensions of the fabricated test pieces are shown in Table 1. Both water and ethanol were used as the coolants in the single-phase experiments. Various micropumps and power levels were tested in the experiments. The different micropumps used in the experiments are listed in the Table 2. The heat transfer capabilities of the cooling system with different pipe diameters and working mediums were also evaluated. The influence of the pumping flow rate and test system on the cooling performance was analyzed experimentally.

Table 2 Specifications of the micropumps

ID	Input voltage (V)	Current draw (A)	Power usage (W)	Pressure head (m)	Pipe inner diameter (mm)
I	8–24	1.9	3–33	3.1	12
II	12	0.4	4.8	1.5	6
III	3–4.5	0.28–0.42	1.89	1.1	3.2

Figure 8 shows the relation between heat sink substrate temperatures and volumetric flow rates under the same input heating power for heat sink I and micropump I. Here, the input power was 80 W. The temperature of the inlet water into the heat sink was kept at 21.2°C in all tests. It can be seen that the substrate temperature decreases as the flow rate increases. When the flow rate of the micropump was 885 mL/min, the substrate temperature was nearly 39.2°C. However, when the flow rate decreased to 52 mL/min, the substrate temperature increased to about 80°C.

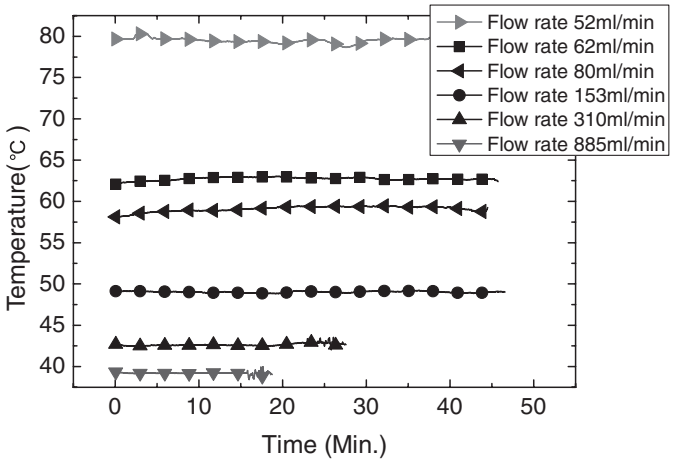

Figure 8 Variation of heat sink substrate temperatures with time at different flow rates under 80 W heating power.

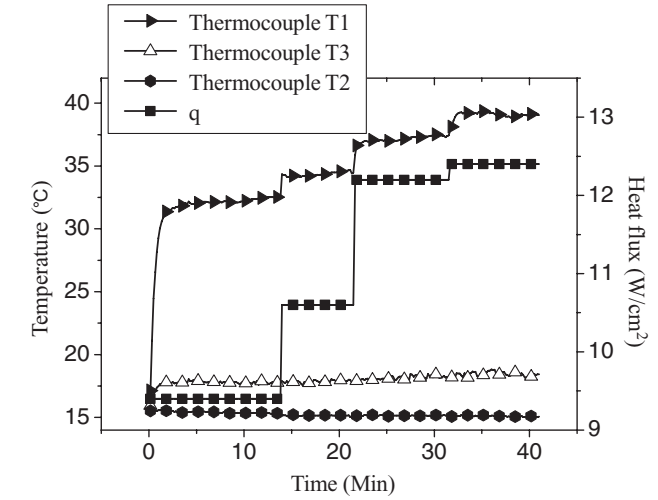

（a）Heating power : 80W, 90W, 100W, 110W

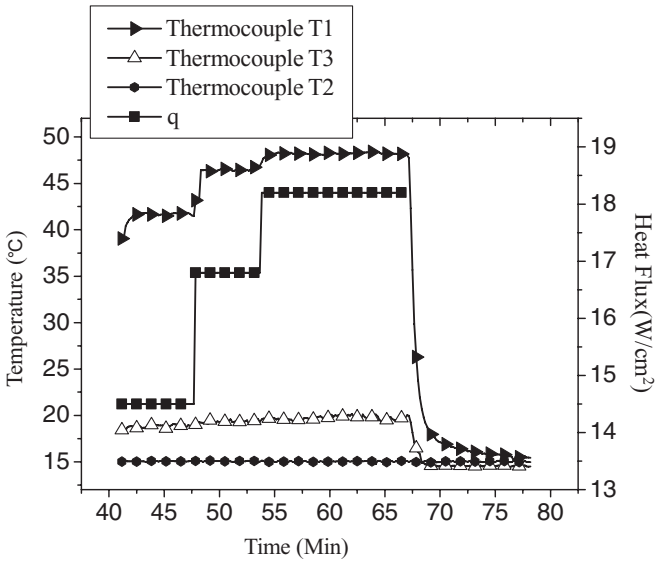

（b）Heating power :120W, 140W, 150W, no heating

Figure 7 Temperature variation with time at different heating power.

It is easy to explain this phenomenon. When the pump flow rate increases, the heat transfer coefficient in the microchannel heat sink increases as well, and thus the heat from the heater is more efficiently removed. However, it should be noticed that as the pump flow rate increases, the micropump will consume more power, which increases the operation cost. Under actual operation, there will be some trade-off in design between the efficiency of heat transfer and power consumption.

Figure 9 shows the variation of heat sink substrate temperatures with input heating power at different inlet water temperatures of heat sink I and micropump II. Here, tests were conducted at two different inlet water temperatures with average flow rates of 298 mL/min and 322 mL/min. The substrate temperatures increased with the rise of the input heating power. When the inlet temperature was 21.2°C and the flow rate 288 mL/min, the substrate temperature was about 50.4°C under 110 W input heating power, and increased to 61.1°C as the heating power rose to 140 W and 129 W. When the inlet temperature was 18.1°C and the flow rate was 321 mL/min, the substrate temperature was about 47.4°C at 110 W of input heating power and increased to 57.4°C as the heating power rose to 140 W and 136 W.

The influence of different heat sink design on the substrate temperature with the input heating power under the same pumping power is shown in Figure 10. Heat sink II had a larger honeycomb cell ex-circle diameter of 2.49 mm and a smaller seal region of 1 mm than 2.27 mm and 3 mm of the heat sink I. The inner diameters of inlet and outlet pipe of the heat sink II were 4 mm, also larger than 2 mm of the heat sink I. More details of the two types of heat sinks are shown in Table 1. Using the same micropump II and pumping power of 2.4 W (12 V, 0.2 A), two types of heat sinks were tested under the same inlet water temperature of 16.2°C and the input heating power. It is very

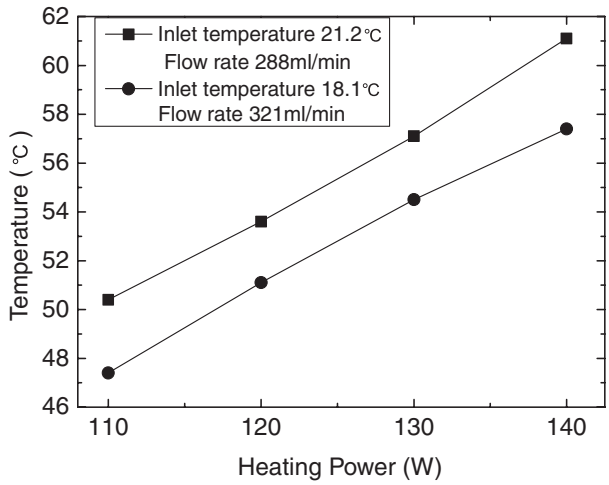

Figure 9 Variation of heat sink substrate temperatures with input heating power at different inlet temperatures.

clear from Figure 10 that the flow rate of heat sink II was much greater than that of heat sink I, shown in the decreased flow resistance present in heat sink II because of the larger honeycomb cells and the diameters of the in/out pipes. When the diameters of the heat sink's inlet and outlet pipes were less than the ones of micropump, the capability of the liquid to flow through was decreased because the pipe diameters of heat sink I and micropump II did not match. For the cooling system, the substrate temperature was 47.2°C for heat sink I at 110 W input heating power, 5°C higher than the substrate temperature for heat sink II. When the heating power rises to 130 W, the substrate temperature of heat sink I increases to 52.8°C, 7°C higher than that of heat sink II, as shown in Figure 10.

Heat transfer tests of the cooling system using heat sink II were also conducted at low inlet temperatures and small liquid

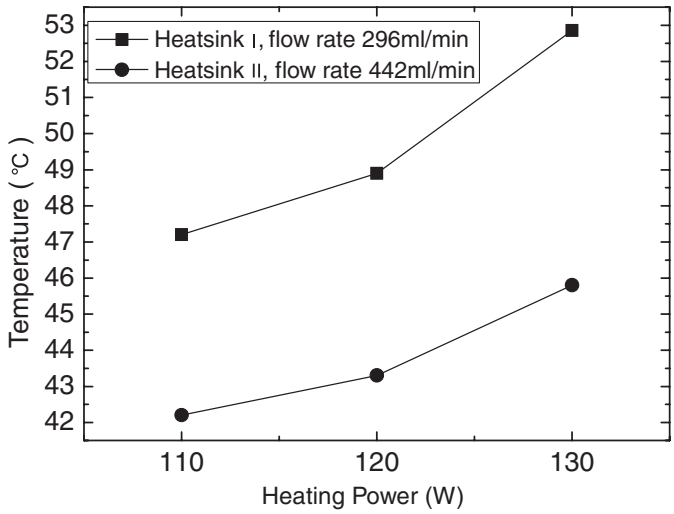

Figure 10 Variation of heat sink substrate temperatures with input heating power at different heat sink design under same pumping power.

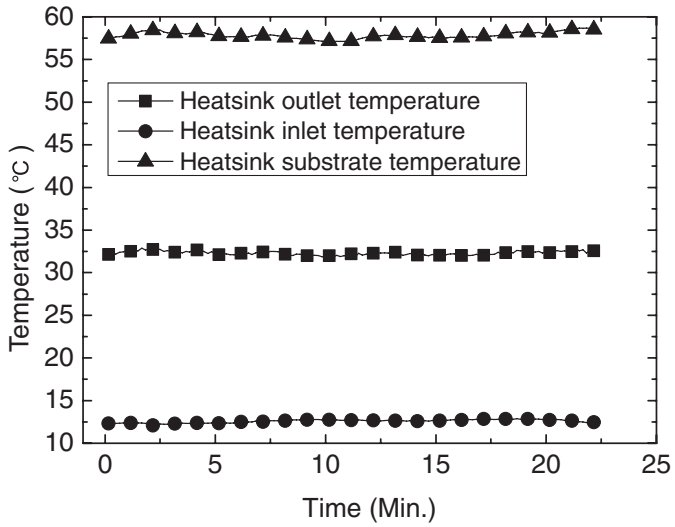

Figure 11 Variation of heat sink temperatures with time under 110 W heating power (micropump III, water).

flow rates. Here, the heat exchanger in system was a cold plate attached to the chilling water unit, with the design being similar to that of a radiator in space applications. The present radiator was created using an aluminum alloy plate of 350 × 255 × 7 mm. A stainless-steel pipe with an inner diameter of 2 mm and length of 2 m was embedded into this cold plate. Another 2-m length of the same stainless-steel pipe was used to connect the heat sink and the radiator. Working fluids such as water and ethanol were driven by micropump to transfer the input heating power to the radiator. Figure 11 shows the temperature variation of heat sink II with time at 110W heating power. In this test, water was used as the working liquid, driven by Micropump III, which consumed 1.12 W pumping power. The inlet and outlet temperatures were 12.6°C and 32.3°C. The substrate

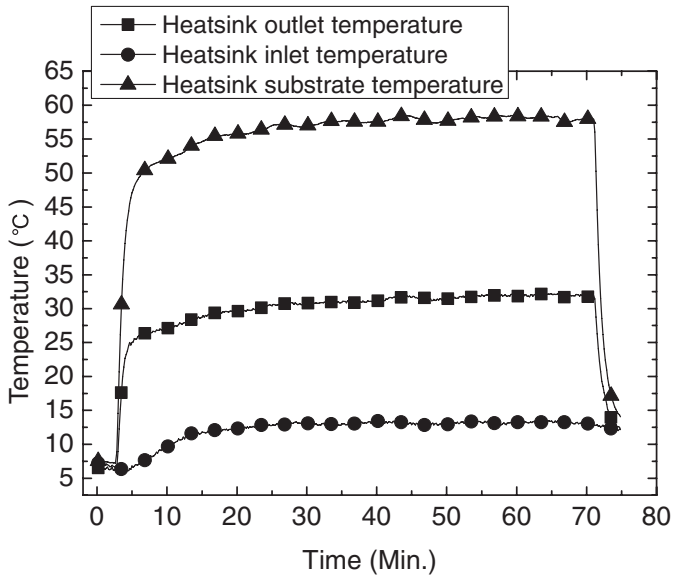

Figure 12 Heat sink temperature variation with time under 80 W heating power (two sets of micropump III in series, ethanol).

temperature was about 57.8°C. When ethanol was used in the cooling system as a working fluid, two sets of micropump III were connected in the series to provide higher pumping capability, with a total of 2.24 W pumping power consumed to push the working fluid. Figure 12 shows the temperature variation of heat sink II with time at 80 W heating power. Here we can see that the substrate temperature increased very quickly when heating was begun. As the inlet temperature rose from 6.7°C to the stable temperature of 13°C, the outlet and substrate temperatures were kept at 31.8°C and 58.2°C. Comparing Figure 11 with Figure 12, it was found that the water system had a better cooling performance compared to the ethanol ones. According to Eq. (1), under the conditions of the same mass flow rate $\dot{m}$ and temperature change ΔT, the total heat transfer rate $\dot{Q}$ by fluid has a linear relation to the specific heat of the fluid c_p. The specific heat of water is 4.183 kJ/kg-K, which is much higher than the specific heat of ethanol at 2.382 kJ/kg-K. This shows that fluids with a high specific heat and low viscosity ratio are more suitable for use in the present cooling system.

CONCLUSIONS

A practical implementation of a single-phase brass honeycomb porous microchannel cooling system was developed for cooling electronic chips. Metal etching was used for the fabrication, and cooling fluid flows in and out from the top of the cascaded plates with staggered honeycomb cells. Preliminary experimental investigation was conducted to understand the characteristics of heat transfer and cooling performance under steady single-phase flow. The heat transfer capabilities of the cooling system using different pipe diameters, different working media, and various pumping powers were also evaluated. The influence of working flow rates and test systems on the cooling performance was also analyzed experimentally. The experimental results show that the cooling system can effectively and efficiently remove the heat flux of 18.2 W/cm^2 at 2.4 W of pumping power. The heat sink design provides a good option for cooling electronic chips. Improved cooling capabilities of the system rely not only on increasing the pump power, but also on matching the pump diameters and system pipe sizes. The physical properties of the working fluid and its mass flow rate are also important to system performance. Further experimental and theoretical investigations are necessary to understand the present system.

NOMENCLATURE

a	seal region width around the microchannel plate perimeter, m
A	area of the bottom wall of the microchannel heat sink, m^2
c_p	specific heat, kJ/kg-K
d	honeycomb cell ex-circle diameter, m
D	inner diameter of heat sink pipe, m
H	microchannel plate thickness, m
I	electronic current, A
L	microchannel plate length, m
$\dot{m}$	total mass flow rate, kg/s
n	number of microchannel plates
P	input power, W
q	heat flux at the bottom wall of the microchannel heat sink removed by water, W/m^2
$\dot{Q}$	heat transfer rate removed by water, W
t	honeycomb cell thickness, m
T	temperature, K
ΔT	change in temperature, K
V	voltage, V
$\dot{v}$	total volumetric flow rate, m^3/s
W	microchannel plate width, m

REFERENCES

[1] Tuckerman, D. B., and Pease, R. F. W., High-Performance Heat Sinking for VLSI, *IEEE Electronic Device Letters*, EDL-2, no. 5, pp. 126–129, 1981.

[2] Phillips, R. J., Microchannel Heat Sinks, *ASME Conference: Advances in Thermal Modeling of Electronic Components and Systems*, New York, vol. 2, pp. 109–184, 1990.

[3] Sasaki, S., and Kishimoto, T., Optimal Structure for Micro-Grooved Cooling Fin for High-Power LSI Devices, *Electronic Letters*, vol. 22, no. 25, pp. 1332–1334, 1986.

[4] Steinke, M. E., and Kandlikar, S. G., Single-Phase Heat Transfer Enhancement Techniques in Microchannel and Minichannel Flows, *Proceedings of the Second International Conference on Microchannels and Minichannels*, Rochester, NY, June 17-19, pp. 141–148, 2004.

[5] Kandlikar, S. G., and Upadhye, H. R., Extending the Heat Flux Limit With Enhanced Microchannels in Direct Single-Phase Cooling of Computer Chips, *IEEE-Semi-Therm, 21*, San Jose, CA, March 15–17, pp. 8–15, 2005.

[6] Lu, T. J., Heat Transfer Efficiency of Metal Honeycombs, *International Journal of Heat and Mass Transfer*, vol. 42, pp. 2031–2040, 1999.

[7] Evans, A. G., Hutchinson, J. W., and Ashby, M. F., Multi-Functionality of Cellular Metal Systems, *Progress in Materials Science*, vol. 43, pp. 171–221, 1999.

[8] Lu, T. J., Valdevit, L., and Evans, A. G., Active Cooling by Metallic Sandwich Structures With Periodic Cores, *Progress in Materials Science*, vol. 50, pp. 789–815, 2005.

[9] Tian, J., Lu, T. J., Hodson, H. P., Queheillalt, D. T., and Wadley, H. N. G., Cross Flow Heat Exchange of Textile Cellular Metal Core Sandwich Panels, *International Journal of Heat and Mass Transfer*, vol. 50, pp. 2521–2536, 2007.

[10] Wen, T., Tian, J., Lu, T. J., Queheillalt, D. T., and Wadley, H. N. G., Forced Convection in Metallic Honeycomb

Structures, *International Journal of Heat and Mass Transfer*, vol. 49, pp. 3313–3324, 2006.

[11] Hayes, A. M., Wang, A., Dempsey, B. M., and McDowell, D. L., Mechanics of Linear Cellular Alloys, *Proceedings of IMECE 2001, International Mechanical Engineering Congress and Exposition, American Society of Mechanical Engineers, New York*, 2001.

[12] Dempsey, B. M., Eisele, S., and McDowell, D. L., Heat Sink Applications of Extruded Metal Honeycombs, *International Journal of Heat and Mass Transfer*, vol. 48, pp. 527–535, 2005.

[13] Exel, K. and Schulz-Harder, J., Water Cooled DBC Direct Bonded Copper Substrates, *IECON '98. Proceedings of the 24th Annual Conference of the IEEE,* Aachen, Germany, Aug 31–Sep.4, vol. 4, pp. 2350–2354, 1998.

Xiaobing Luo is a professor at the Huazhong University of Science and Technology (HUST), Wuhan, China. He works at the State Key Lab of Coal Combustion in School of Energy and Power Engineering and Wuhan National Lab for Optoelectronics in HUST. He received his Ph.D. in 2002 from Tsinghua University, China. From 2002 to 2005, he worked at Samsung Electronics in Korea as a senior engineer. In September 2005, he returned to China and became an associate professor. In October 2007, he was promoted to full professor. His main research interests are LED packaging, electronics packaging, heat and mass transfer, and MEMS sensors and actuators. He has published more than 50 papers, and applied for and owns 40 patents in the United States, Korea, Japan, Europe, and China.

Yonglu Liu is a Ph.D. student at the Huazhong University of Science and Technology (HUST), Wuhan, China. He also works at the Nanchang Institute of Technology in Nanchang, China. He received his M.S. degree in mechanical engineering from HUST. His main research interests are heat and mass transfer and micro cooling.

Wei Liu is a professor at the Huazhong University of Science and Technology (HUST), Wuhan, China. He works at the School of Energy and Power Engineering in HUST. His main research interests are heat and mass transfer. He has published more than 100 papers, and applied for and owns 10 patents in China.